

Research article

The role of film composition and nanostructuring on the polyphenol sensor performance

Cibely Silva Martin, Mateus Dassie Maximino, Matheus Santos Pereira, Clarissa de Almeida Olivati, and Priscila Alessio *

Departamento de Física, Faculdade de Ciências e Tecnologia, UNESP Univ. Estadual Paulista, Presidente Prudente, SP, Brazil, 19060-900.

* **Correspondence:** Email: prialessio@gmail.com; Tel: +55-18-32295751.

Abstract: The recent advances in the supramolecular control in nanostructured films have improved the performance of organic-based devices. However, the effect of different supramolecular arrangement on the sensor or biosensor performance is poorly studied yet. In this paper, we show the role of the composition and nanostructuring of the films on the impedance and voltammetric-based sensor performance to catechol detection. The films here studied were composed by a perylene derivative (PTCD-NH₂) and a metallic phthalocyanine (FePc), using Langmuir-Blodgett (LB) and physical vapor deposition (PVD) techniques. The deposition technique and intrinsic properties of compounds showed influence on electrical and electrocatalytic responses. The PVD PTCD-NH₂ shows the best sensor performance to the detection of catechol. Quantification of catechol contents in mate tea samples was also evaluated, and the results showed good agreement compared with Folin-Ciocalteu standard method for polyphenol detection.

Keywords: nanostructuring; PVD films; LB films; phthalocyanine; perylene, polyphenol sensor

1. Introduction

One of the challenges in the chemistry of materials is to achieve control over the structuration of molecules to enhance devices performance or driven to new applications [1,2,3]. In this context,

supramolecular organization plays an important role in sensors performance. For instance, in the work of Volpati et al. [4] the role of the ultrathin film architecture composed by phthalocyanines in the sensing unit performance was exploited. That work revealed that a sensor array could be built using sensing units with identical or similar materials changing the architectures of the ultrathin films.

Sensors based on nanostructured films are assembled from many different fabrication techniques on the nanoscale. Techniques known to produce films with nanostructured architectures in solid substrates are Langmuir, Langmuir-Blodgett, Langmuir-Schaefer, Layer-by-Layer, thermal evaporation between other [5–8]. These techniques allow the formation of thin films of organic molecules including extended π -conjugated ring systems, as phthalocyanines [1,9,10], and perylene derivatives [9,11,12,13], forming organized structures and superstructures driven by π - π -stacking interactions [1,9]. Both molecules, phthalocyanines, and perylenes are interesting to applications in electric and electrochemical sensors due to the noncovalent assemblies of π -conjugated chromophores owing to π - π interaction impacting the percolated pathways for charge transport [2].

Based on the dependence of sensors performance in function of molecular organization and nanostructuring of films composed by phthalocyanine and perylene, we explore the possibility of generating films from iron phthalocyanine (FePc) and n-butylimidoethylenamine perylene (PTCD-NH₂) with distinct electrical and electrochemical properties. The formation of the films was performed using Langmuir-Blodgett (LB) and physical vapor deposition (PVD) deposition techniques, while the properties and sensing application were evaluated using electrical impedance under interdigitated electrodes (IDE) (electrical properties), and differential pulse voltammetry (DPV) under ITO glass electrode (electrochemical properties). The sensorial performance was carried out in the presence of standard catechol solution, and the real application was evaluated in tea sample to polyphenol quantification.

2. Materials and Methods

2.1. PVD and LB films deposition

The molecular structure of both materials used here, iron phthalocyanine (FePc) (Kodak) and n-butylimidoethylenamine perylene (PTCD-NH₂) (provided by Dr. J. Duff from the Xerox Research Center of Canada) are shown in Figure 1. The PVD films of FePc and PTCD-NH₂ were fabricated in a Boc Edwards vacuum system model Auto 306. The powders were placed into a metallic Ta boat. The depositions were carried out by an electrical current at 10^{-6} torr, being the thickness controlled by a quartz crystal microbalance.

The LB films were grown in a KSV Langmuir trough model 2000. The Langmuir films of FePc were formed using a chloroform solution 0.5 mg/mL and deposited at a surface pressure of 25 mN/m, and PTCD-NH₂ were formed using a trifluoroacetic/chloroform (1:10) solution with 0.15 mg/mL and deposited at a surface pressure of 30 mN/m. Both films were obtained by the symmetric compression of the barriers at 10 mm/min with ultrapure water in the subphase.

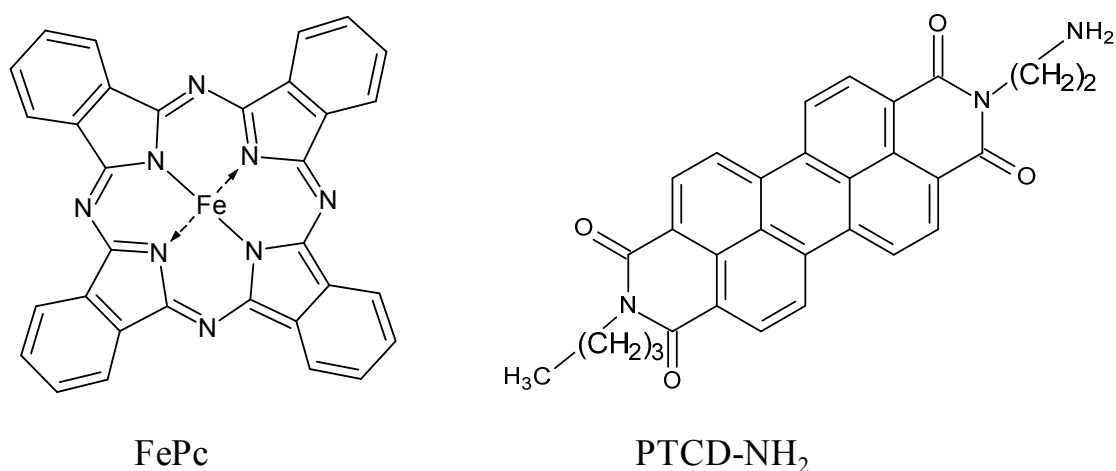


Figure 1. representation of the molecular structure of iron phthalocyanine (FePc) and n-butylimidoethylenamine perylene (PTCD-NH₂).

2.2. Films characterization

The role of film composition and nanostructuring on the impedance performance was evaluated using an assembly composed of four Pt interdigitated electrodes (IDE) covered with films produced with both materials, FePc and PTCD-NH₂ using LB (5 layers) and PVD (10 nm) techniques. The approximate thickness of 5 LB layers is 9 nm for FePc and 15 nm for PTCD-NH₂. The Pt IDE contains 50 pairs of digits, each digit presenting 10 μm in width, 5 mm in length and 100 nm in height, spaced 10 μm each other. The impedance spectroscopy was carried out using an impedance analyzer (Solartron 1260A). The frequency range considered was 80 Hz to 1 MHz and, applied signal with 50 mV of amplitude. The IDE modified units were immersed in ultrapure water and also in 1 μM catechol standard solution (Sigma -Aldrich Brazil).

The role of film composition and nanostructuring on the electrochemical behavior was also evaluated using ITO electrode covered with films produced with FePc and PTCD-NH₂ using LB (5 layers) and PVD (10 nm) techniques. The electrochemical behavior was carried out using a potentiostat/galvanostat μ-autolab type III (EcoChimie). The electrochemical measurements were performed using the differential pulse voltammetry (DPV) applying a potential range of -1.0 to +1.0 V vs. Ag/AgCl, 50 mV of pulse amplitude, and 10 mV/s of scan rate. The measurements were performed using a voltammetric cell of three electrodes, with Ag/AgCl saturated 3M KCl as a reference electrode, a platinum wire as a counter electrode and ITO covered with the PVD or LB films as working electrode. The voltammograms were obtained in supporting electrolyte (0.1 mol/L KCl) and also in 120 μM catechol standard solution.

The roughness for all films deposited onto quartz substrate was estimated using atomic force microscopy (AFM). The measurements were performed out in a Nanosurf microscope model Easyscan2 in tapping mode and resolution of 1024 dots/line.

2.3. Analytical curve

The PVD PTCd-NH₂ film was used to obtain the analytical curve for catechol detection. The analytical curves were obtained by impedance spectroscopy and DPV. The analytical curve from impedance spectroscopy was obtained through the addition of 1.0×10^{-9} , 3.0×10^{-9} , 6.0×10^{-9} , 1.0×10^{-8} , 3.0×10^{-8} , 6.0×10^{-8} , 1.0×10^{-7} , 5.0×10^{-7} and 1.0×10^{-6} mol/L catechol standard solution, while from DPV was obtained through addition of 2×10^{-6} , 4×10^{-6} , 8×10^{-6} , 1.2×10^{-5} , 2×10^{-5} , 4×10^{-5} , 6×10^{-5} , 8×10^{-5} , 1.2×10^{-4} , and 1.6×10^{-4} mol/L catechol standard solution. The electrical impedance technique (absence of supporting electrolyte) is more sensitive than electrochemical techniques. Thus, a high concentration of the analyte produces a saturation of the impedance-based sensor response (interdigitated electrodes). On the other hand, the electrochemical measurements show a response to catechol oxidation only above of 1 μ mol/L.

2.4. Real sample

The PVD PTCd-NH₂ film was applied as a sensor to detect the polyphenol content in mate tea sample. The tea sample was prepared by weighing 1.5 g of herb and adding 100 mL of ultrapure water, heating at 90 °C for 15 minutes with constant stirring (300 rpm). The mate tea sample was filtrated (hot filtration) and the volume adjusted to 100 mL with ultrapure water. The polyphenol determination by impedance spectroscopy and DPV were performed using a 0.002% and 1% (v/v) of the tea extract, respectively.

2.5. Fittings parameters

Equivalent electric circuits can model impedance curves. Z-View software package (Scribner Associates, Southern Pines, NC, USA) was employed for the equivalent circuit fitting. The models of equivalent circuit models for IDEs sensors illustrated in Figure 2 were applied for fitting the impedance spectra. The first equivalent circuit presented in Figure 2(a) was used for spectra fitting when only one semicircle appears in a spectrum at high frequencies, and the low frequency part of the Nyquist plot is quite linear. When the IDEs systems showed spectra with two semicircles, the second equivalent circuit was used to fit them, as presented in Figure 2(b). The parameter R_s represents the bulk solution resistance according to Randles Model. The parallel combination of the C_g - R_{ct} represents the geometrical capacitance of the IDE sensor and the charge transfer resistance of the films layer. In series with the first RC parallel circuit, the second RC composed by a constant phase element, CPE, and R2 present the capacitance and resistance at the interface between the film and the solution [14]. The CPE was modelled as a non-ideal capacitor given by $CPE = -1/(Ci\omega)^\alpha$; where C is the capacitance which describes the charge separation at the double layer interface, ω is the frequency (rad/s) and α exponent associated with the heterogeneity of the electrode surface ($0.5 < \alpha < 1$). In this circuit, the addition of CPE on the circuit is necessary, which can be ascribed to blocking of the diffusion process, once the impedance measurements are made in ultrapure water (absence of electrolyte). Thus, the charge separation occurs, and the interface acts as a non-ideal capacitor (CPE) [15].

Fit precision is assessed through the chi-square parameter which is the sum of squares of the ratio of the standard deviation between the original data and the calculated spectrum. For all spectra showed in this work, the chi-square parameter was smaller than 5.6×10^{-4} .

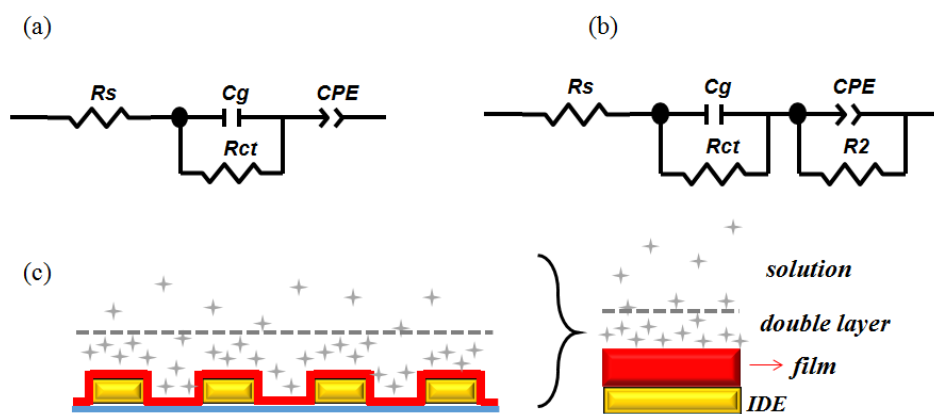


Figure 2. electrical equivalent circuit fitted to IDE bare (a), and IDE covered with films (b). (c) Scheme illustrating each physico-chemical process included in the model.

3. Results and Discussion

3.1. Electrical impedance characterization

The effect of the thin film composition and nanostructuring on the performance of sensors based on impedance spectroscopy was first evaluated in ultrapure water. Figure 3 shows the impedance results of the LB and PVD films for both materials and bare IDE immersed in ultrapure water regarding Bode ($|Z|$ vs. frequency) and Nyquist (Z' vs. Z'') plot.

The impedance spectra profiles of both materials are similar for PVD and LB films. Furthermore, the profile found here is similar to that found by Yang working with the detection of Salmonella cell suspensions in deionized water using gold interdigitated microelectrodes [16]. This impedance spectrum profile (Bode plot) is typically found in systems where the polarization is due to a combination of kinetic and diffusion processes [16]. Comparing the Bode plot for all films studied, the major differences are observed to the PTCN-NH₂ film. The different impedance values for the same material in the form of PVD and LB films are related to the molecular organization of these materials when processed in different ways. For instance, as discussed in Volpati et al. [4], FePc presents an orientation almost parallel to the substrate (between 0° and 45°) in LB film and a preferred orientation perpendicular to the substrate (45° to 90°) in PVD film. For PTCN-NH₂, the molecules are oriented at an angle of approximately 45° with the substrate in PVD films and rather more inclined (> 45°) when in LB films (unpublished results). The important point is that the conductivity is greatly affected by materials that present anisotropy in the molecular orientation. For instance, in the work of Dey and Pal [5], the growth of LbL films of NiTsPc under a magnetic field were studied. Their result shows that the magnetic field induces a preferential molecular orientation on the LbL films of NiTsPc and this change in orientation was responsible for the observed changes

in conductivity values and dielectric constant films. According to Dey and Pal [5], films in which the molecules were immobilized with the macrocycle orientation parallel to the substrate had lower values of dielectric constant and conductivity. Note that in the case of Dey and Pal [5], the electrical devices have been made in Sandwich-Al ITO. This effect is explained by the authors due to the very close packing of the molecules to each other, and the process of electronic conduction occurring in the molecule to molecule is improved. The authors also suggest that when the molecules are oriented perpendicular to the substrate surface, and the macrocycle in a particular direction, the electronic conduction by hopping still prevails compared with films in which the molecules have no specific orientation or organization [5].

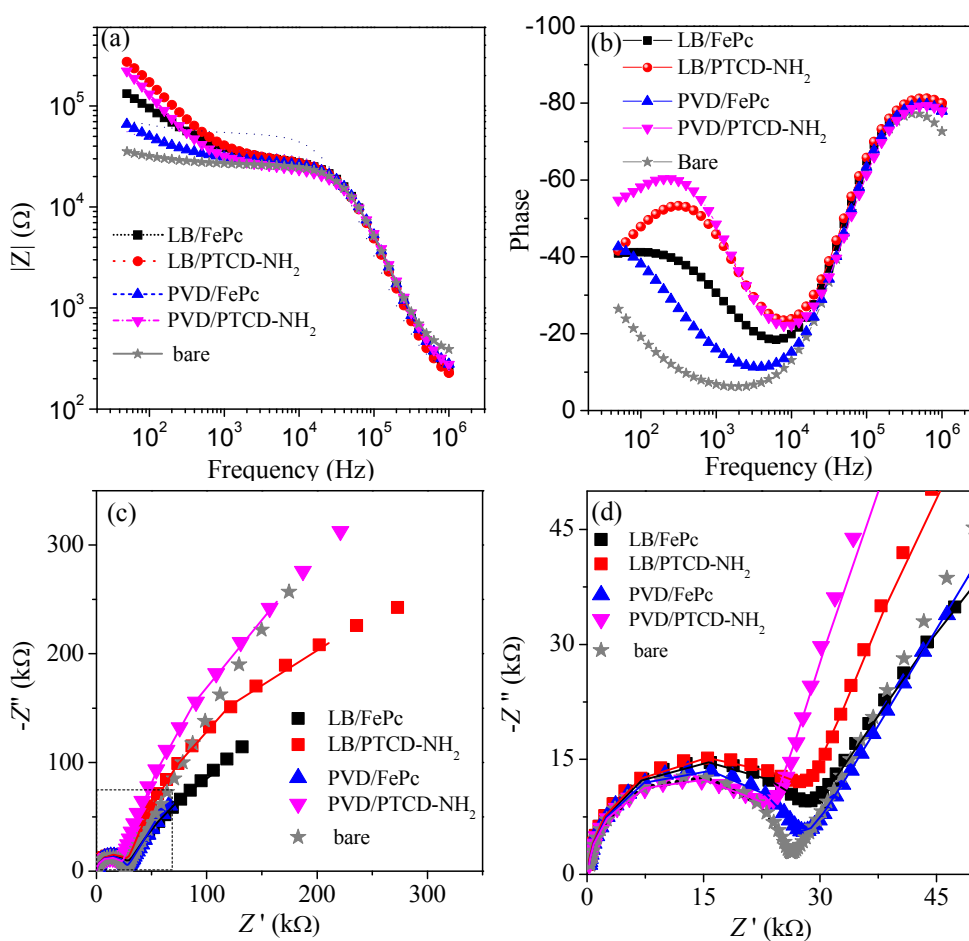


Figure 3. Impedance spectra of IDE bare and IDE covered with PVD and LB films immersed in ultrapure water using Bode plot impedance (a) and phase (b), Nyquist plot (c) and the magnification of the high-frequency range (d) from the plot (c). The solid lines represent fitted data using the equivalent circuits.

Besides, all PVD and LB films promote an increase in the impedance for lower frequencies (~ 50 kHz), as seen in the Bode plot (Figure 3(a)). The order in the impedance values is $\text{LB/PTCD-NH}_2 > \text{PVD/PTCD-NH}_2 > \text{LB/FePc} > \text{PVD/FePc}$. In the low frequencies range (< 100 Hz), impedance related to the double layer (C_d) appear in the spectra and contributes to the impedance value in a

frequency-dependent manner: $Z = -j/\sqrt{2\pi fC}$, where C is capacitance and f is frequency. In this way, the major C_d is presented by the FePc films. The double layer capacitance is attributed to the reversible ion adsorption onto the film surface, which gives rise to an electrolyte/film interface, where no faradaic (redox) processes are involved. This capacitance can be described according to $C = \varepsilon A/d$, where ε is the electrolyte dielectric constant, A is the film surface area accessible to ions, and d is the distance between the center of the ion and film surface. Thus, once in our case, the same electrolyte was used, higher values of C_d could be related to two mainly factors: i) larger surface areas promoted by porous (or aggregated) films and ii) shorter distances between ion-surface promoted by the material characteristic.

All impedance spectra show a semicircle in the high frequency range (kinetic control of the charge-transfer process) and a quite linear range at a lower frequency (diffusion control) in Nyquist plots. The impedance spectrum of bare IDE electrode was modeled using the equivalent circuit in Figure 2(a). The impedance spectra of the IDEs coated with films were modeled using the equivalent circuit in Figure 2(b). In the presence of film on IDE surface, a resistance parameter was added in comparison with the equivalent circuit from the bare. The first RC parallel can be associated with the charge transfer equilibrium at IDE surface, once that the circuit parameters show no significant changes between the films (Table 1). However, the second RC parallel showed significant changes, suggesting an influence of the films on diffusion process. These differences in circuit parameters for the same material in the form of PVD and LB films are related to the molecular organization of these materials when processed in different ways. Moreover, in the FePc case, the roughness decreases from 10.27 nm to 1.4 nm from the LB to PVD films. This decrease of roughness can be ascribed to FePc characteristic in aggregates itself through π - π interaction in solution [17], which are transferred to Langmuir films. Thus, the PVD technique which uses solid compound produces more homogeneous surface during the film deposition. Based on molecular organization and surface roughness the PVD technique allows a molecular orientation that favors the insertion of water molecules on the FePc films, increasing the CPE values.

Table 1. Parameters obtained from equivalent circuit fitting from impedance measurements in ultrapure water and roughness of the IDE bare and IDE covered with PVD and LB films.

Film	R_{Ω}/Ω	$C/\mu\text{F s}^{\alpha-1}$	R_{ct}/Ω	$\text{CPE}/\mu\text{F s}^{\alpha-1}$	α	R_2/Ω	Roughness/nm
Bare	301.7	1.30×10^{-10}	25122	1.15	0.65	-	
LB/FePc	117.4	1.35×10^{-10}	26080	0.0828	0.70	4.19×10^5	10.27
PVD/FePc	175.1	1.28×10^{-10}	26141	0.267	0.68	1.00×10^6	1.4
LB/PTCD-NH ₂	131.9	1.35×10^{-10}	26471	0.0169	0.82	6.27×10^5	4.10
PVD/PTCD-NH ₂	188.7	1.33×10^{-10}	22363	0.0164	0.84	1.01×10^6	2.00

The PTCD-NH₂ films showed small variation not only on the molecular organization (between 45° and 90°) but also on roughness. The latter being from 4.10 nm to 2.00 nm for LB and PVD films, respectively. In agreement with the impedance results obtained to FePc films, the PTCD-NH₂ showed the similar tendency, being the PVD films more homogeneous than LB films. Thus we can conclude that molecular organization of thin films on substrate surface influences directly on impedance properties in ultrapure water.

After impedance analysis in ultrapure water, the nanostructured films measurements in standard catechol solution were done to investigate the influence of the different composition and molecular orientation of the thin films as impedance sensor. The IDEs modified with LB and PVD films were immersed in 1.0×10^{-6} mol/L catechol standard solution. All films showed decreases of a semicircle, ascribed to increases of charge transfer on the electrode surface (Figure 4). The results indicate the LB and PVD films from FePc and PTCD-NH₂ showed interaction with catechol molecules. The equivalent circuit modeled in this situation was the same that applied to films immersed in ultrapure water. However, the R_{ct} decreases as expected, which can be ascribed to the increase of charge transfer between the film and catechol molecules, increasing the conductivity of the system. The greatest decrease of the semicircle diameter (R_{ct}) in catechol solution was observed to PVD PTCD-NH₂ films, indicating the best sensitivity. This sensitivity is an interesting property to the sensor application. Thus, the PVD PTCD-NH₂ sensor was used to evaluate the sensing performance in low catechol concentrations.

Table 2. Parameters obtained from equivalent circuit fitting from impedance measurements in catechol solution of the IDE bare and IDE covered with PVD and LB films.

Film	R_Q/Ω	$C/\mu\text{F s}^{\alpha-1}$	R_{ct}/Ω	$CPE/\mu\text{F s}^{\alpha-1}$	α	R_2/Ω
LB/FePc	124.5	1.35×10^{-10}	22322	0.0734	0.71	4.66×10^5
PVD/FePc	183.5	1.27×10^{-10}	23068	0.284	0.68	1.10×10^6
LB/PTCD-NH ₂	136.3	1.34×10^{-10}	22429	0.0162	0.83	5.87×10^5
PVD/PTCD-NH ₂	189.4	1.33×10^{-10}	19763	0.0168	0.84	8.99×10^5

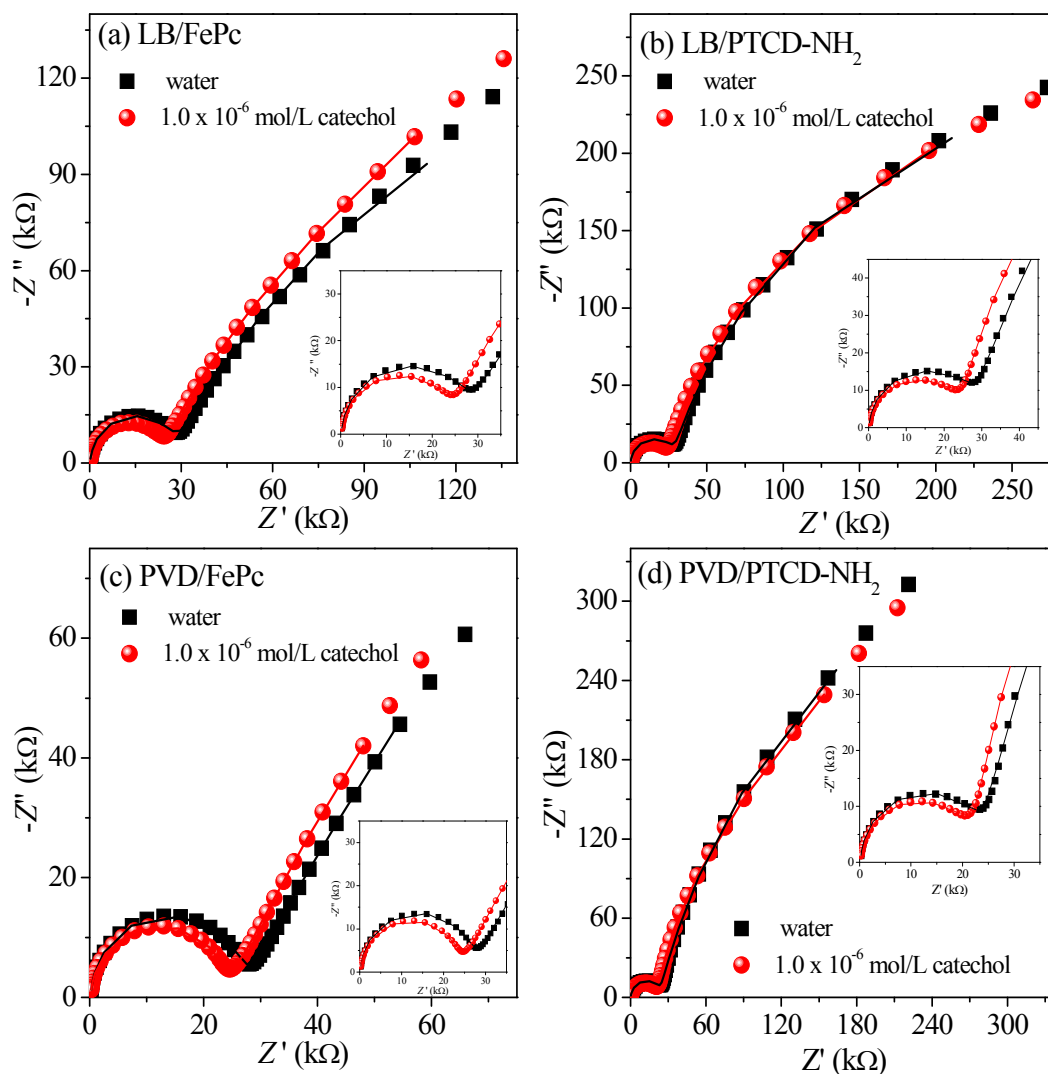


Figure 4. Nyquist plot of IDE with PVD and LB films immersed in ultrapure water (square curve) and 1.0×10^{-6} mol/L catechol solution (circle curve). Lines indicates equivalent circuit fitting. *Inset:* magnification of the high-frequency range.

The impedance measurements were performed using catechol concentrations in ultrapure water: 1.0×10^{-9} , 3.0×10^{-9} , 6.0×10^{-9} , 1.0×10^{-8} , 3.0×10^{-8} , 6.0×10^{-8} , 1.0×10^{-7} , 5.0×10^{-7} and 1.0×10^{-6} mol/L. The increases of catechol concentration promote increases of charge transfer observed through the decreases semicircle diameter (decreases of R_{ct}). The curve of $1/R_{ct}$ in function of catechol concentration showed an exponential dependence, as showed at Figure 5. Linearity can be observed from 1.0×10^{-9} to 1.0×10^{-6} mol/L, with linear regression of $1/R_{ct}$ ($1/\Omega$) = $2.09255 \times 10^{-5} + 2.09002 \times 10^{-6}$ [catechol].

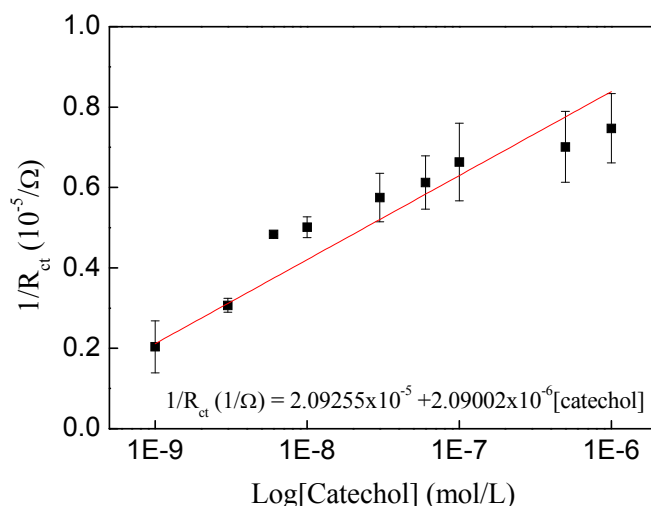


Figure 5. response of the PVD PTCD-NH₂ impedance sensor in ultrapure water containing different catechol concentrations. Measurements performed to three different electrodes (average from measurements in triplicate).

3.2. Differential pulse voltammetry

The results from voltammetric measurements collaborate with the results observed from impedance in ultrapure water. The films formed by PVD technique showed better stability and voltammetric signal in supporting electrolyte (0.1 mol/L KCl). The redox potential observed in negative range (Figure 6) can be ascribed to ring oxidation of perylene or phthalocyanine ligand [18,19]. The electrodes immersed in catechol solution (Figure 6) showed a peak potential ascribed to catechol oxidation [20], which showed a shift of oxidation potential to lower potential in comparison with ITO electrode uncovered (catechol oxidation at 0.231 V vs. Ag/AgCl). The small catechol oxidation potential was observed to PVD films, being 0.046 and 0.076 V vs. Ag/AgCl for PTCD-NH₂ and FePc films, respectively. The potentials for catechol oxidation are summarized in Table 3. The PDV films are more homogeneous than LB films, suggesting like as in impedance behavior, the homogeneity can influence on the electrocatalytic effect of this films. The increase of homogeneity and the decreases of roughness observed from PVD to LB films decrease the onset potential of catechol oxidation.

Table 3. Potential of catechol oxidation using PTCD-NH₂ and FePc films.

Film	E_{ox} (V) vs. Ag/AgCl
Bare	0.231
PVD/PTCD-NH ₂	0.046
LB/PTCD-NH ₂	0.167
PVD/FePc	0.076
LB/FePc	0.195

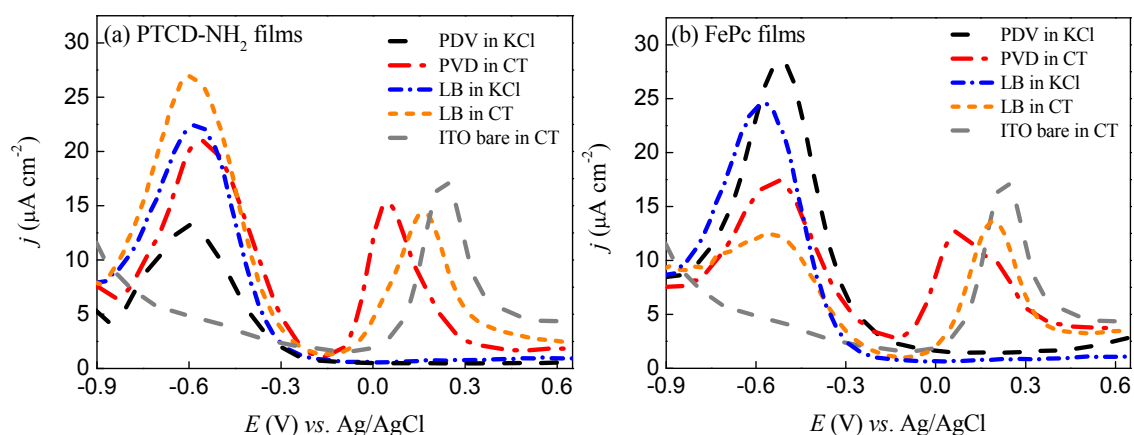


Figure 6. differential pulse voltammograms of PVD and LB PTCD-NH₂ films (a), and PVD and LB FePc films (b) immersed in supporting electrolyte (0.1 mol/L KCl) and standard catechol solution (1.2×10^{-4} mol/L). The voltammogram of ITO bare in catechol solution also is shown.

Also, the thickness of PVD films showed influence on film oxidation but has no influence on catechol peak oxidation (supporting information). This behavior reinforces the hypothesis that the interaction of catechol occurs on the film surface, which promotes a fast saturation of films surface/signal principally observed on impedance measurements.

The voltammetry in agreement with impedance results collaborates with the hypothesis that molecular organization of thin films on substrate surface influences directly on electrochemical and electrical properties of the films. Thus, the results from DPV and impedance measurements suggesting PTCD-NH₂ films showed the better potential (i.e. smaller potential to catechol oxidation) for the development of sensor devices to the determination of catechol and/or polyphenols derivatives.

The PVD PTCD-NH₂ films were also used to evaluate the electrochemical sensing performance. The DPV measurements were performed using 2×10^{-6} , 4×10^{-6} , 8×10^{-6} , 1.2×10^{-5} , 2×10^{-5} , 4×10^{-5} , 6×10^{-5} , 8×10^{-5} , 1.2×10^{-4} and 1.6×10^{-4} mol/L catechol standard solution. The anodic peak current at 0.046 V vs. Ag/AgCl (ascribed to catechol oxidation) increase linearly with the catechol concentration from 2.0×10^{-6} to 1.6×10^{-4} mol/L (Figure 7). The linear regression equation can be represented by $I_{pa} \text{ (A)} = 1.956 \times 10^{-7} + 0.2516 [\text{catechol mol/L}]$ ($r = 0.998$), with limit of detection (LOD) of 1.62×10^{-7} mol/L (0.162 $\mu\text{mol/L}$) calculated according to $3 \times \text{SD/slope}$ criteria.

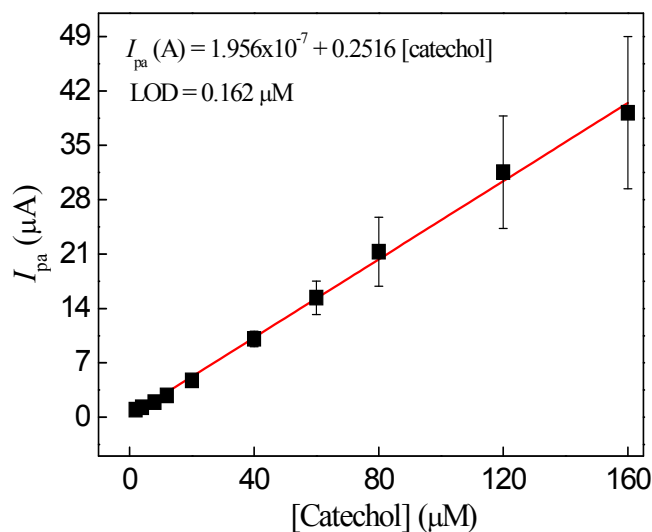


Figure 7. response of the PVD PTCD-NH₂ voltammetric sensor in KCl solution for different catechol concentrations. Measurements performed in triplicate using the same electrode, and three different electrodes as well (average of nine addition measurements).

The analytical performance of PVD PTCD-NH₂ was similar or better than other sensors and biosensor as summarized in Table 4. The PVD PTCD-NH₂ films show a satisfactory limit of detection to the application as catechol sensor.

Table 4. Comparison of analytical performance of sensors for the detection of catechol.

Film	Detection technique	Linear range (μmol/L)	LOD (μmol/L)	Ref.
Tyr/AA/LuPc ₂	Cyclic voltammetry	1.67-21.46	1.71	[20]
(PAH/FeTsPc+ DPPG/AgNp) ₅	Cyclic voltammetry	2.0-100	0.87	[21]
PEDOT/CPE	DPV	1.0-250	0.50	[22]
Polypyrrol/AuNp	Cyclic voltammetry	0.1-1.0	3-88	[23]
3-APBA-PTCA-CNTs/GC	DPV	0.5-30	0.10	[24]
PVD PTCD-NH ₂	DPV	2-160	0.16	This work

Abbreviation: Tyr = tyrosine enzyme; AA = arachidic acid; LuPc₂ = lutetium phthalocyanine; PAH = poly (allylamine) hydrochlorate; FeTsPc = iron tetrasulfonated phthalocya-nine; DPPG = phospholipid 1,2-dipalmitoyl-sn-3-glycero-(phosphor-rac-(1-glycerol); AgNp = silver nanoparticles; PEDOT = poly(3,4-ethylenedioxythiophene); CPE = carbon past electrode; AuNp = gold nanoparticles; APBA-PTCA = 3-aminophenylboronic acid-3,4,9,10-perylene tetracarboxylic acid; CNTs = carbon nanotubes, GC = glassy carbon.

3.3. Analyses in mate tea samples

PVD PTC₂D-NH₂ films were applied as a sensor to determine the catechol content in mate tea samples using electrical impedance and DPV methods. The catechol concentration in mate tea sample was determined using standard addition in both analytical methods. The catechol concentrations in mate tea samples determined by DPV measurements was 171.3 mg/L (± 15.6), while the value determined using impedance measurements was 0.09 mg/L (± 0.13). Comparing with the value found using Folin-Cioaltea method (297 mg/L ± 8.5), a standard method for polyphenol quantification, DPV method showed higher efficiency than impedance method. The results for polyphenols quantification are summarized in Table 4.

The impedance measurements are very sensitive to the variation on interface IDE surface/solution. Thus, the complex tea sample matrix showed a higher influence on charge transfer with leading to an error on catechol quantification. Besides, an adsorption of polyphenols and the other compounds present in tea matrix can occur. The poisoning or “memory effect” can be observed through comparison of the impedance response in the initial ultrapure water (before measurements in catechol) and final ultrapure water (after measurements in catechol) in Figure 8. As is shown below for PTC₂D-NH₂, the impedance profile changes due to the catechol adsorption. This effect was not observed in the electrochemical measurements. Thus, in this case, the electrical impedance cannot be used as an analytical method using the PVD PTC₂D-NH₂ films.

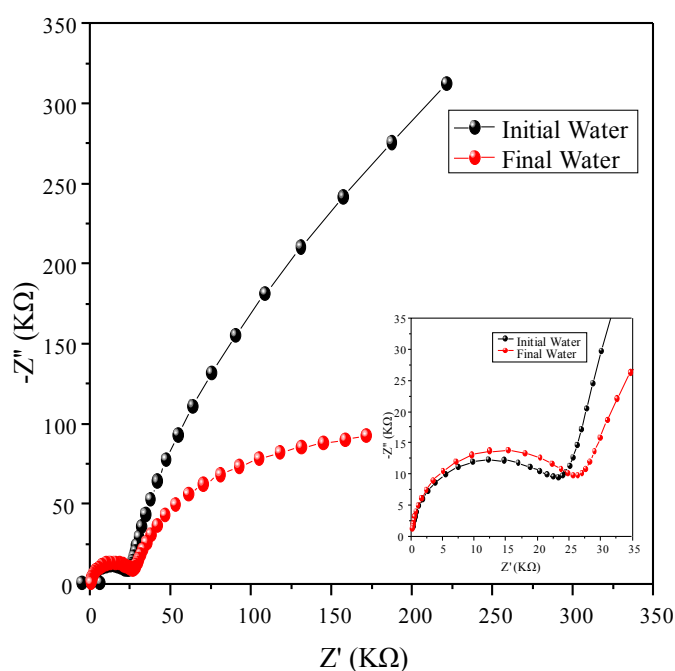


Figure 8. Nyquist plot of IDE with PTC₂D-NH₂ PVD film immersed in ultrapure water before (initial water) and after (final water) catechol measurements.

However, using DPV method the concentration found was close to that determined by the standard method. The difference observed are assigned to oxidation potential used in DPV the

measurements. The maximum peak potential for the mate tea sample using PDV PTCN-NH₂ films was observed at 0.205 V vs. Ag/AgCl (1% of tea), and to catechol oxidation at 0.046 V vs. Ag/AgCl. The oxidation peak observed in the tea sample can be ascribed to oxidation of epicatechin flavan-3-ol derivatives[25]. The mate tea sample showed higher levels of EC than other flavan-3-ol. Thus, the values found in this work include only polyphenols oxidized around 0.046 V.

Table 4. Polyphenol quantification in mate tea sample.

Method*	Amount of polyphenol (mg/L)
Differential pulse voltammetry	171.3 (±15.6)
Electrical impedance	0.090 (±0.13)
Folin-Ciocalteu	297.0 (±8.50)

*the differential pulse voltammetry and electrical impedance were applied using PDV PTCN-NH₂ films.

4. Conclusion

The Langmuir-Blodgett and physical vapor deposition techniques allow the formation of thin films from FePc and PTCN-NH₂ compounds with different molecular organization and nanostructuring. Molecular organization and nanostructuring directly influenced the electrical and electrochemical properties of these films. The impedance results in ultrapure water showed the films onto IDE modified the electrical response. In general, equivalent circuits reveal an increase in the resistance of the system in the low frequency range with the films deposition, associated with the diffusional process. Comparing LB and PVD films, the PDV deposition promotes more homogeneous films and with lower roughness. These characteristics favor the insertion of water molecules, increasing the CPE values. The same tendency was observed in catechol solution, once PDV films better interact with catechol molecules. The latter was analyzed by the decreasing of resistance values in high and low frequency range. The electrocatalytic properties were also evaluated by using differential pulse voltammetry for films deposited onto ITO electrode. Both PVD films (FePc and PTCN-NH₂) showed smaller onset potential for catechol oxidation in comparison with LB films, which can be directly associated with the molecular organization, homogeneity, and roughness. However, the thicknesses not show significant influence.

These observations agree with impedance results, which confirm nanostructuring play an important role on electrical and electrochemical properties of this films (principally in catechol solution). Among FePc and PTCN-NH₂ films (LB and PVD), the PVD PTCN-NH₂ film showed interesting electrical and electrochemical properties for the application as catechol sensor. The analytical curve for catechol detection was obtained using PVD PTCN-NH₂ film through impedance and DPV methods. The impedance signal showed an exponential dependence with low catechol concentration, indicating a sensitive interaction on IDE interface. However, the voltammetric signal was linear with catechol concentration with a limit of detection of 1.62×10^{-7} mol/L. The PVD PTCN-NH₂ film was tested as a sensor for quantification of catechol contents in mate tea samples. Using

DPV method the concentration of catechol found (171.3 mg/L) was close to that determined by the Folin-Cioaltea standard method.

Acknowledgments

This work was supported by FAPESP, CNPq, and CAPES.

Conflict of Interest

All authors declare no conflicts of interest in this paper.

References

1. Engelkamp H, Middelbeek S, Nolte JMR, et al. (1999) Self-Assembly of Disk-Shaped Molecules to Coiled-Coil Aggregates with Tunable Helicity. *Science* 284: 785–788.
2. Mondal T, Basak D, Al Ouahabi A, et al. (2015) Extended supramolecular organization of [small pi]-systems using yet unexplored simultaneous intra- and inter-molecular H-bonding motifs of 1,3-dihydroxy derivatives. *Chem Commun* 51: 5040–5043.
3. Lu H, Kobayashi N (2016) Optically Active Porphyrin and Phthalocyanine Systems. *Chem Rev* 116: 6184–6261.
4. Volpati D, Alessio P, Zanfolim AA, et al. (2008) Exploiting Distinct Molecular Architectures of Ultrathin Films Made with Iron Phthalocyanine for Sensing. *J Phys Chem B* 112: 15275–15282.
5. Dey S, Pal AJ (2011) Layer-by-Layer Electrostatic Assembly with a Control over Orientation of Molecules: Anisotropy of Electrical Conductivity and Dielectric Properties. *Langmuir* 27: 8687–8693.
6. Eccher J, Zajaczkowski W, Faria GC, et al. (2015) Thermal Evaporation versus Spin-Coating: Electrical Performance in Columnar Liquid Crystal OLEDs. *ACS Appl Mater Interface* 7: 16374–16381.
7. Cea P, Ballesteros Luz M, Martín S (2014) Nanofabrication techniques of highly organized monolayers sandwiched between two electrodes for molecular electronics. *Nanofabrication*.
8. Camacho SA, Aoki PHB, Assis FFd, et al. (2014) Supramolecular arrangements of an organometallic forming nanostructured films. *Mater Res* 17: 1375–1383.
9. Yang Y, Zhang Y, Wei Z (2013) Supramolecular Helices: Chirality Transfer from Conjugated Molecules to Structures. *Adv Mater* 25: 6039–6049.
10. Li W-S, Aida T (2009) Dendrimer Porphyrins and Phthalocyanines. *Chem Rev* 109: 6047–6076.
11. Chen Z, Lohr A, Saha-Moller CR, et al. (2009) Self-assembled [small pi]-stacks of functional dyes in solution: structural and thermodynamic features. *Chem Soc Rev* 38: 564–584.
12. Würthner F (2004) Perylene bisimide dyes as versatile building blocks for functional supramolecular architectures. *Chem Commun* 1564–1579.
13. Würthner F, Thalacker C, Diele S, et al. (2001) Fluorescent J-type Aggregates and Thermotropic Columnar Mesophases of Perylene Bisimide Dyes. *Chemistry–A Eur J* 7: 2245–2253.

14. Voitechovič E, Bratov A, Abramova N, et al. (2015) Development of label-free impedimetric platform based on new conductive polyaniline polymer and three-dimensional interdigitated electrode array for biosensor applications. *Electrochim Acta* 173: 59–66.
15. Bisquert J, Garcia-Belmonte G, Bueno P, et al. (1998) Impedance of constant phase element (CPE)-blocked diffusion in film electrodes. *J Electroanal Chem* 452: 229–234.
16. Yang L (2008) Electrical impedance spectroscopy for detection of bacterial cells in suspensions using interdigitated microelectrodes. *Talanta* 74: 1621–1629.
17. Bertoncello P, Peruffo M (2008) An investigation on the self-aggregation properties of sulfonated copper(II) phthalocyanine (CuTsPc) thin films. *Colloid Surface A* 321: 106–112.
18. Lee SK, Zu Y, Herrmann A, et al. (1999) Electrochemistry, Spectroscopy and Electrogenerated Chemiluminescence of Perylene, Terrylene, and Quaterylene Diimides in Aprotic Solution. *J Am Chem Soc* 121: 3513–3520.
19. Arıcı M, Arıcan D, Uğur AL, et al. (2013) Electrochemical and spectroelectrochemical characterization of newly synthesized manganese, cobalt, iron and copper phthalocyanines. *Electrochim Acta* 87: 554–566.
20. Apetrei C, Alessio P, Constantino CJL, et al. (2011) Biomimetic biosensor based on lipidic layers containing tyrosinase and lutetium bisphthalocyanine for the detection of antioxidants. *Biosens Bioelectron* 26: 2513–2519.
21. Alessio P, Martin CS, de Saja JA, et al. (2016) Mimetic biosensors composed by layer-by-layer films of phospholipid, phthalocyanine and silver nanoparticles to polyphenol detection. *Sensor Actuat B-Chem* 233: 654–666.
22. Song Y, Yang T, Zhou X, et al. (2016) A microsensor for hydroquinone and catechol based on a poly(3,4-ethylenedioxythiophene) modified carbon fiber electrode. *Anal Method* 8: 886–892.
23. García-Hernández C, García-Cabezón C, Medina-Plaza C, et al. (2015) Electrochemical behavior of polypyrrol/AuNP composites deposited by different electrochemical methods: sensing properties towards catechol. *Beilstein J Nanotechnol* 6: 2052–2061.
24. Liu W, Wu L, Zhang X, et al. (2014) Highly-selective electrochemical determination of catechol based on 3-aminophenylboronic acid-3,4,9,10-perylene tetracarboxylic acid functionalized carbon nanotubes modified electrode. *Anal Method* 6: 718–724.
25. Janeiro P, Oliveira Brett AM (2004) Catechin electrochemical oxidation mechanisms. *Anal Chim Acta* 518: 109–115.



AIMS Press

© 2017 Priscila Alessio, et al., licensee AIMS Press. This is an open access article distributed under the terms of the Creative Commons Attribution License (<http://creativecommons.org/licenses/by/4.0>)